NASA TECHNICAL MEMORANDUM

NASA TM X-1373

NASA TM X-1373

EXPERIMENTAL STUDY OF DYNAMICS OF MERCURY-VAPOR CONDENSING

by Roland C. Fisher

Lewis Research Center

Cleveland, Ohio

NATIONAL AERONAUTICS AND SPACE ADMINISTRATION • WASHINGTON, D. C. • MAY 1967

NASA-TM-X-1373

EXPERIMENTAL STUDY OF DYNAMICS OF MERCURY-VAPOR CONDENSING

By Roland C. Fisher

Lewis Research Center
Cleveland, Ohio

NATIONAL AERONAUTICS AND SPACE ADMINISTRATION

For sale by the Clearinghouse for Federal Scientific and Technical Information
Springfield, Virginia 22151 – CFSTI price $3.00

EXPERIMENTAL STUDY OF DYNAMICS OF MERCURY-VAPOR CONDENSING

by Roland C. Fisher

Lewis Research Center

SUMMARY

An experimental investigation was conducted to determine the dynamic characteristics of a single-tube mercury-vapor condenser cooled by gas in crossflow configuration. The dynamic studies employed cycling of the inlet-vapor-flow rate to the condenser. Through use of a constant-pressure receiver, the interface location was allowed to vary freely in response to changes in condensing pressure. Simultaneous responses of condenser-inlet pressure and liquid-vapor interface position to an approximately sinusodial variation in vapor-flow rate about a given quiescent level were obtained. The response range investigated was primarily between 0.01 and 1 cycle per second. The responses were presented in the form of Bode plots.

The condenser was observed to have two distinct regions of operation identifiable by a high or a low sensitivity of inlet pressure to interface position. The response of condenser-inlet pressure to vapor-flow rate was observed to be different in each of the regions. In the low-sensitivity region, the frequency response data of condenser pressure to vapor-flow rate indicated an approximate lag-lead-lag characteristic. In the high-sensitivity region, the frequency response data indicated an approximate lead-lag-lag characteristic.

The response of interface position to vapor-flow rate was presented for the region of low sensitivity of inlet pressure to interface position and also for the transition region between high and low sensitivity. An approximate overdamped second-order response was obtained.

The effect of increasing the liquid-pressure drop resulted in the interface response being moved to lower frequencies.

INTRODUCTION

A knowledge of the dynamic characteristics of liquid-metal-vapor condensers is of

practical interest in the design of Rankine cycle power-generating systems for space flight application. Though operation of the condenser at a given design point is generally intended, excursions or disturbances may occur, such as those due to variations in radiator environment or changes in power input from the turbine. Control modes have been proposed to nullify these effects (ref. 1). In postulating these control modes, knowledge of the transfer function form of various condenser variables is necessary, together with the associated numerical values and approximate variation with change in operating point. Though a large amount of technical information relative to heat-exchanger transfer functions is available, information is lacking on the dynamics of heat exchangers wherein metallic vapors are condensed. Accordingly, an experiment on a mercury-vapor condenser was conducted at the Lewis Research Center to obtain basic dynamic information on this power system component. Some of the data from this experiment were reported in reference 2 for the purpose of evaluating a theoretical analysis of condenser dynamics. The present report is a more detailed presentation of the experimental results of the program.

The condenser employed for this experiment was designed to permit the basic dynamic characteristics to be obtained with a minimum of complicating features. The condenser was a single constant-diameter tube, horizontally mounted, and cooled by gas in crossflow configuration. The purpose of the experiment was to obtain dynamic-pressure information relative to a disturbance in inlet-vapor-flow rate. Dynamic information was also obtained on the attendant change in interface location (liquid inventory). The interface moved freely in response to condensing pressure changes since a constant-pressure receiver was used at the condenser outlet. Electronic circuitry was devised to provide an approximate analog-type signal for recording of interface location.

Cycling of the inlet valve was employed to provide sinusoidal variations in inlet-vapor-flow rate. The resulting dynamic data, normalized to steady-state condenser operation, is presented in the form of Bode plots (i.e., log amplitude and phase shift as a function of log frequency). With such plots, of course, transfer functions can be readily determined.

SYMBOLS

K proportionality constant in vapor venturi flow calculation

P_R total pressure in receiver, psia

ΔP_M differential pressure of nitrogen cooling gas (i.e., manifold pressure less chamber pressure), psi

ΔP_{1-2} differential pressure drop across calibrated orifice at outlet of expulsion reservoir, psi

P_5 static pressure in the plenum outlet channel, psia

P_6 static pressure just ahead of venturi, psia

ΔP_{6-7} differential pressure drop between P_6 station and throat of venturi, psi

P_7 analog calculated value of venturi throat static pressure, $P_7 = P_6 - \Delta P_{6-7}$, psia

P_8 static pressure at venturi outlet, taken as condenser-inlet pressure, psia

$\overline{P_8}$ averaged P_8 pressure reading during cyclic operation, psia

ΔP_8 differential change in P_8 reading from its quiescent level (for cyclic variations it corresponds to peak-to-peak value), psi

ΔP_9 differential pressure drop across outlet valve, psi

T_{27} total temperature at P_6 station, ^{o}F

ΔVT differential change in VT reading from its quiescent level (for cyclic variations it corresponds to peak-to-peak value), percent

W_L liquid-mercury-flow rate from expulsion reservoir into the system, lb/sec

W_N flow rate of nitrogen cooling gas into manifold, lb/sec

W_V vapor-flow rate into condenser as indicated by venturi measurements, lb/sec

$\overline{W}_V$ averaged vapor-flow rate into condenser during cyclic operation, lb/sec

ΔW_V differential change of vapor-flow rate from its quiescent level (for cyclic variations it corresponds to peak-to-peak value), lb/sec

ΔW_{VC} equal to $\Delta W_V/(\overline{W}_V/W_L)$, applied when the value of $\overline{W}_V$ slightly exceeds that of W_L, lb/sec

$\Delta W'_{VC}$ high-frequency values of ΔW_{VC} as corrected for resonance effect in test rig, lb/sec

APPARATUS AND INSTRUMENTATION

Test Rig

The arrangement of the experimental system is presented schematically in figure 1. A supply of liquid mercury was contained in a large expulsion reservoir. This reservior was equipped with an adjustable pressure regulator through which the steady-state flow level could be established. Monitoring of this flow level was accomplished by passing

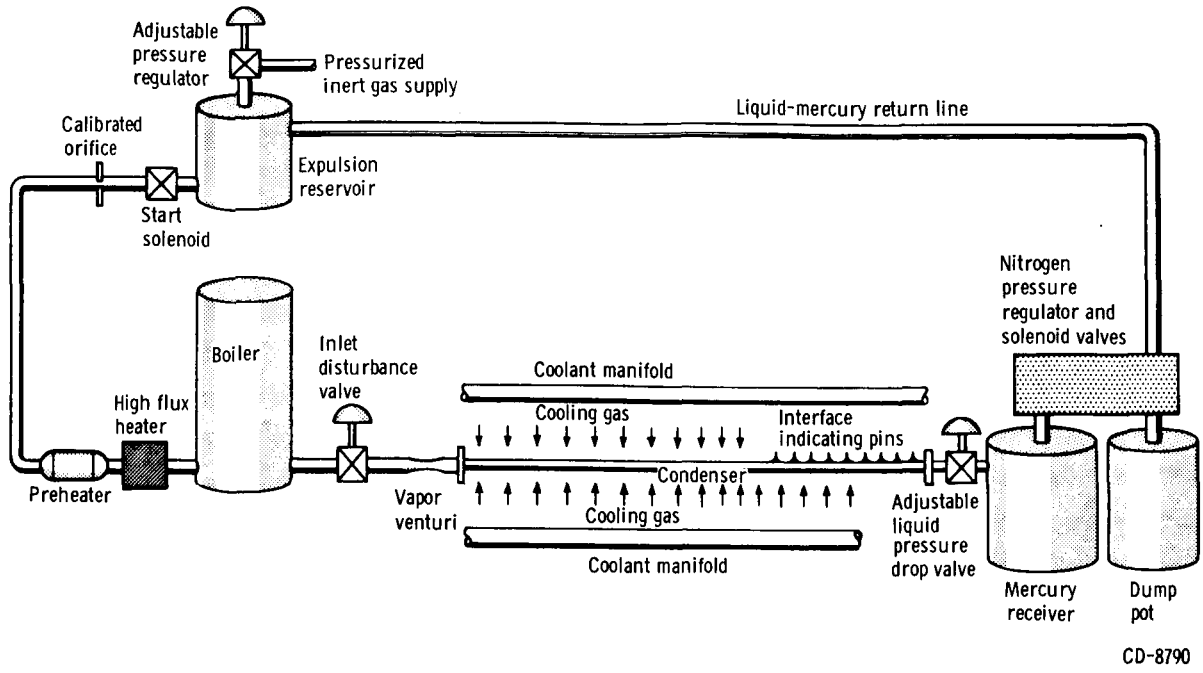

Figure 1. - Basic schematic of test rig.

the reservoir's outlet flow through a calibrated orifice. Following the orifice, the liquid mercury was raised approximately to the boiling point with a preheater. From the preheater the mercury passed to a high-heat-flux unit, which produced a low quality vapor. The vapor was then passed into a main boiler where its quality approached 100 percent. A large plenum was incorporated inside the main boiler helix in order that cyclic flow variations could be made with negligible disturbance to the boiler operation and at the same time could have sufficient accumulator action to allow cycling to very low frequencies at a substantially constant pressure level. Following this plenum, the mercury vapor passed through an inlet disturbance valve. The resultant instantaneous flow was monitored with a calibrated vapor venturi. The vapor then entered the condensing tube wherein its latent heat of vaporization was rejected, and the liquid was subcooled before passing through an adjustable valve at the condenser outlet. From the outlet valve, the condensate then flowed with further subcooling into an adjustable pressure receiver. A dump pot and a network of valves were incorporated with the receiver to allow intermittent return of the liquid mercury, after sufficient accumulation, to the expulsion reservoir without shutting down the system.

The condenser tube was a 90-inch-long constant-diameter stainless-steel tube (0.311-in. i.d. by 0.032-in. wall) mounted horizontally within the rig. At the downstream end of the tube, fusite pins were installed on bosses through the top of the tube wall at 1-inch intervals for purposes of measuring interface location.

Crossflow cooling of the condensing tube was employed by means of nitrogen jets

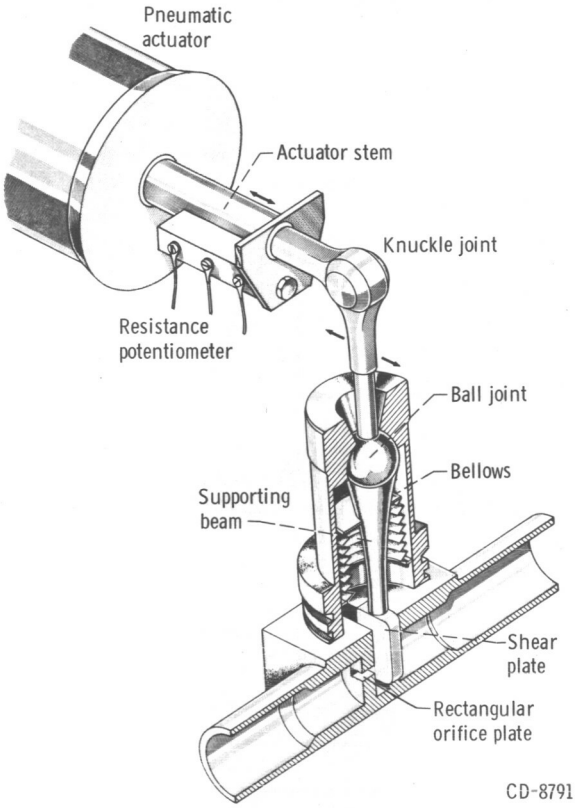

Figure 2. - Vapor-flow valve, linkage, and motion pickoff.

from two diametrically opposed manifolds which paralleled the condenser tube. The flow rate of cooling gas could be set with an adjustable regulator.

Of particular importance to the dynamic studies was the condenser-inlet valve. The valve selected, depicted in figure 2, was a commerical type specifically designed for caustic molten metals and operable to high temperatures. The valve incorporated stainless-steel construction throughout except for the tungsten shear plate, which sweeps between the orifice plates and the stellite shear-plate supporting beam. The valve was sealed by a seamless bellows with the ball joint serving as an emergency seal. The toggling action of the beam results in a minimum of bellows movement, which is desirable for prolonged life under repeated cycling conditions imposed by dynamic studies.

The valve was specified to have narrow rectangular ports so arc-machined into its orifice plates that the open area change would be very nearly linear with arm travel. By operating the valve under choked conditions from a large plenum, sinusoidal variations in valve travel produced nearly sinusoidal variations in inlet-vapor-weight-flow rate. This valve, as well as the plug type condenser outlet valve, was driven by an electropneumatic actuator. As there was negligible hysteresis between input voltage and valve position, the electronic circuit shown in figure 3 was used for valve drive signal preparation. Pneumatic boosters applied to the upstream valve resulted in a flat response to approximately 1 cps with limited attenuation at the higher frequencies.

The condenser and associated hardware previously mentioned were mounted within a steel chamber, shown in figure 4, which was continually purged through a scrubber system during hot operation to reduce the mercury-vapor hazard in the event of spillage. The heating controls, valve controls, instrumentation electronics, and readout and recording systems were mounted external to the chamber.

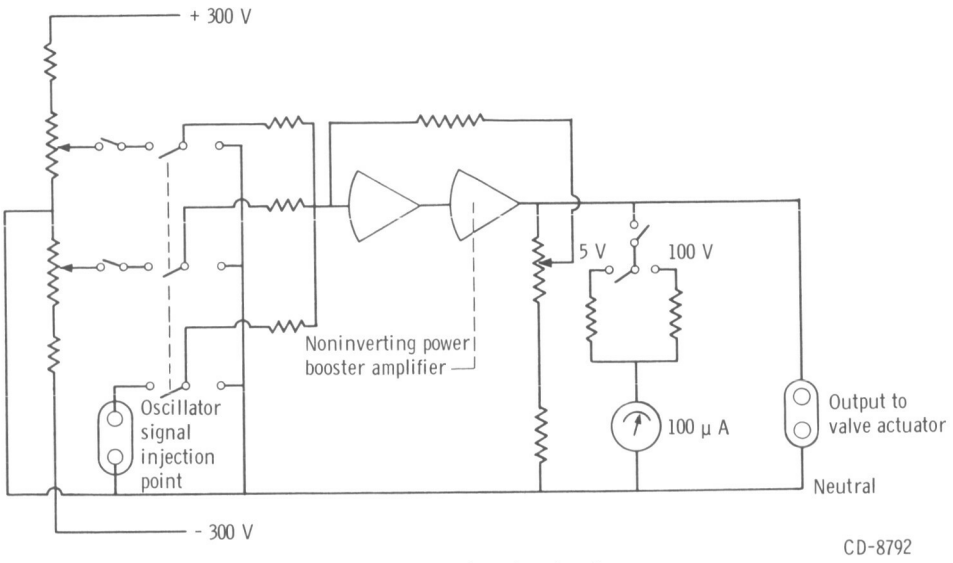

Figure 3. - Valve drive circuit.

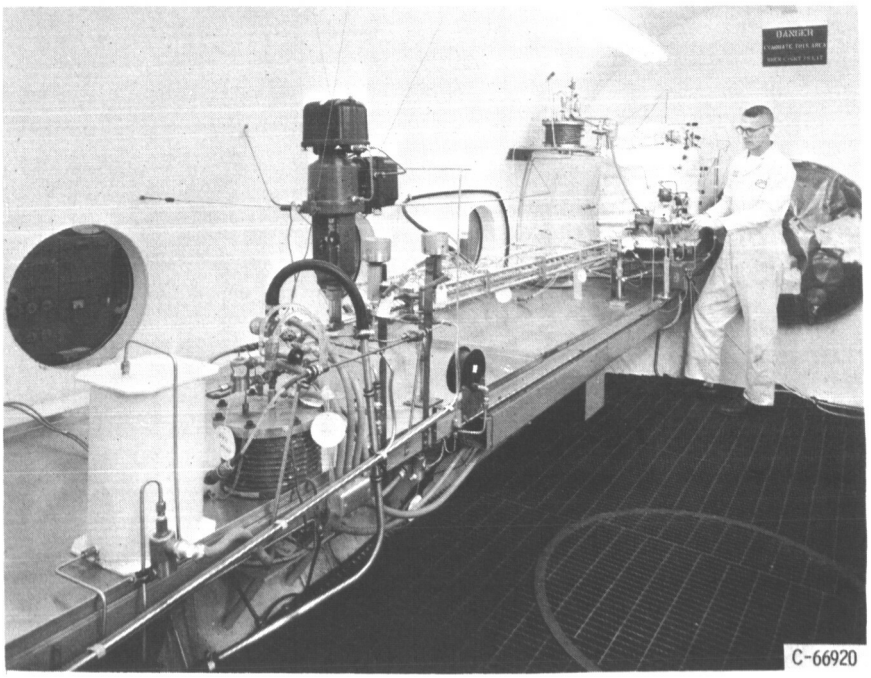

Figure 4. - Test facility.

Instrumentation

The location of instrumentation points is shown in figure 5.

Flow. - Analog computation techniques were applied to the appropriate pressure and temperature measurements in order to furnish instantaneous values of mercury-flow rate. The liquid-mercury-flow rate from the expulsion reservoir into the system was measured by a differential pressure pickup placed across a calibrated orifice (figs. 5 and 6). This orifice was calibrated by weighing a timed amount of flow at a constant differential pressure. The resulting flow - pressure-drop data matched a square-root curve very closely as was expected. The differential pressure signal was modified and displayed on a panel meter at the test site for ease in calibration. Also, the signal was applied to an open operational amplifier which incorporated an unsegmented nonlinear device in its feedback circuit for producing a square-root signal that, when properly scaled, provided a signal proportional to the liquid-mercury flow. The flow rate was read out on a panel meter and was recorded on a channel of an eight-channel strip recorder.

Measurement of the instantaneous vapor-flow rate into the condenser was accomplished by processing pressure and temperature measurements from a calibrated venturi

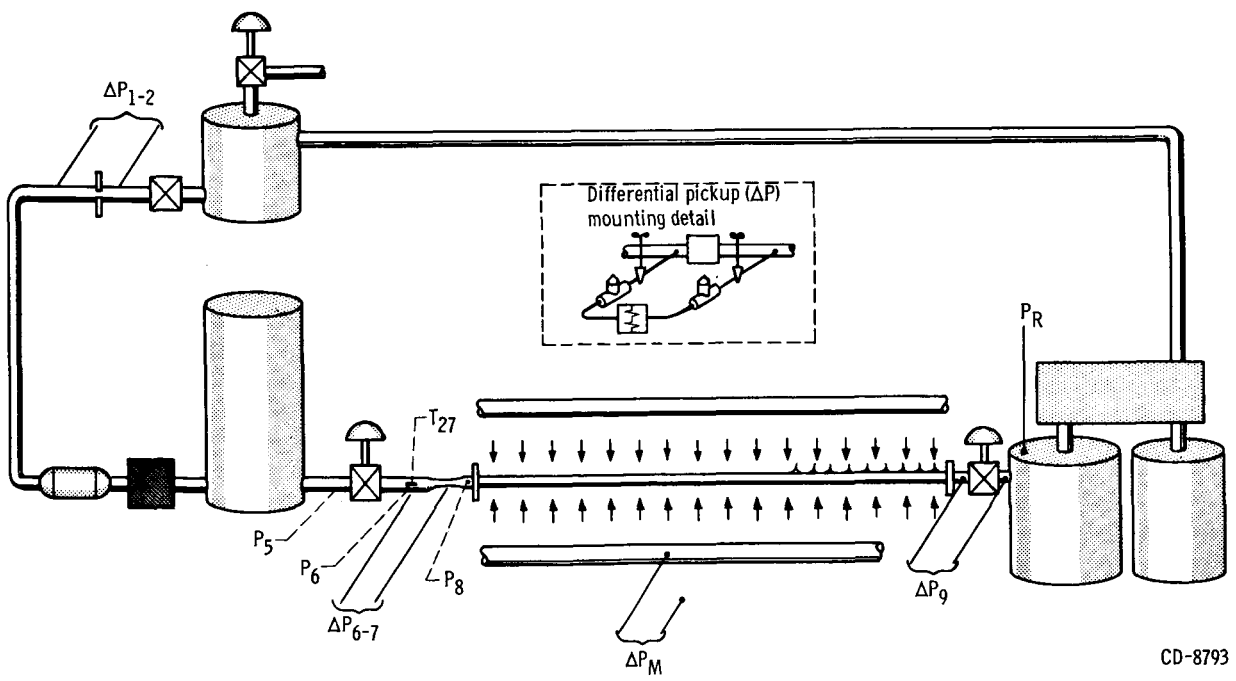

Figure 5. - Location of instrumentation.

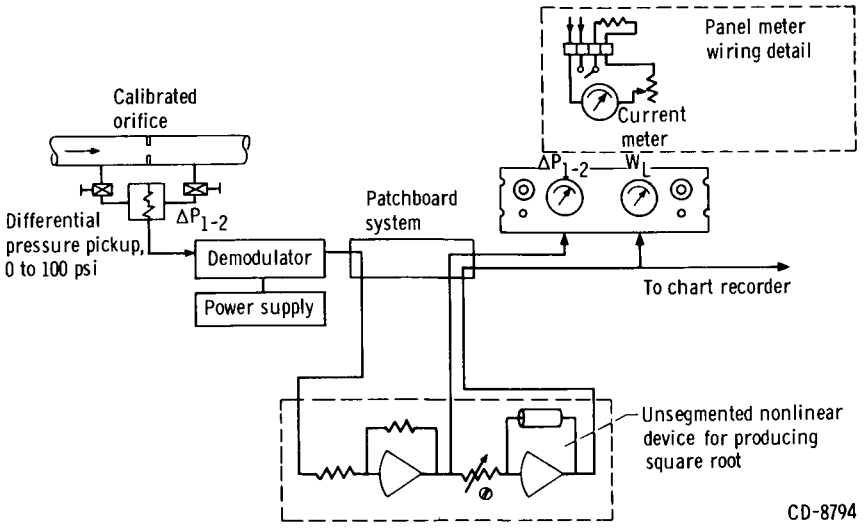

Figure 6. - Measurement of liquid-mercury-flow rate from expulsion reservoir.

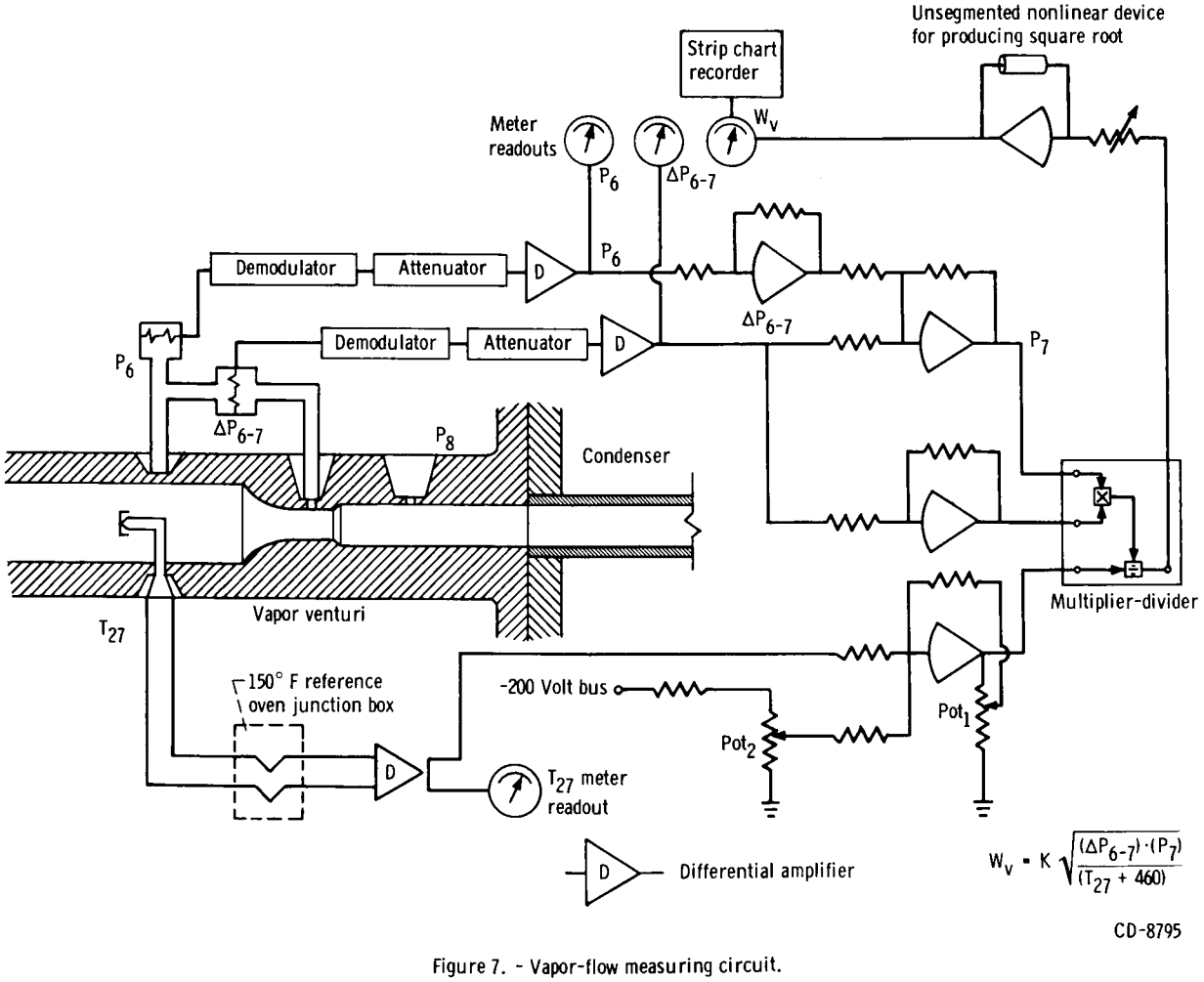

Figure 7. - Vapor-flow measuring circuit.

TABLE I. - METRIC CONVERSION

To convert from	To	Multiply by
psi (lb force/sq in.)	N/sq m	6895
in.	m	0.0254
lb/sec (lb force avoirdupois)	N/sec	4.448
^{o}F	^{o}K	$(5/9)(^{o}F + 459.67)$

as shown in figure 7. Table I gives factors to convert to metric units. The relation used was $W_V = K\sqrt{\Delta P_{6-7} P_7/(T_{27} + 460)}$, which, though a simplified approximation, was suitable for this experiment. The pressure P_7, which is the venturi throat static pressure, was obtained from the relation $P_7 = P_6 - \Delta P_{6-7}$. The pressure transducer for measuring P_6 was a very high-frequency-response flush diaphragm type suitable for high-temperature use. This transducer was mounted horizontally and was closely coupled to the static tap ahead of the venturi section. The pressure pickup for ΔP_{6-7} was of the differential type. A small chambered volume on either side of the diaphragm is inherent with this type of pickup. Also, the differential pickup was not operable to as high a temperature level; therefore, liquid mercury was maintained in the coupling lines by slanting them slightly downward.

To obtain the temperature T_{27}, a sheathed Chromel-Alumel temperature probe approximately 1/16 inch in diameter was inserted in the center of the channel opposite the P_6 station and was bent slightly upstream. A stainless-steel shroud was placed over the thermocouple end to avoid its being wetted by mercury droplets, which would have caused it to read droplet temperature instead of vapor temperature. The thermocouple lines terminated in a 150^{o} F reference oven junction box. Copper lines carried the thermocouple millivolt signal to a high input impedance, high closed-loop gain differential amplifier. The amplified output, at a very low impedance level, was used to drive a meter readout at the operating site. The T_{27} meter movement had its mechanical zero reset to correspond to 150^{o} F, which, of course, matches the reference oven. Analog circuitry was employed to add in a voltage to convert the temperature signal from the 150^{o} F reference base to degrees Rankine. This conversion was done by setting potentiometer pot 2. Potentiometer pot 1, which provided the amplifier in the temperature circuit with an adjustable gain, was used in scaling the temperature signal prior to insertion into the multiplier-divider.

The analog computation of vapor flow was performed as follows: The P_6 signal was inverted and summed with the ΔP_{6-7} signal to form the P_7 signal $P_7 = P_6 - \Delta P_{6-7}$, which was then proportional to the static pressure at the venturi throat. The P_7 and ΔP_{6-7} signals were then multiplied together after which their product was divided by the T_{27} signal which had been converted to degrees Rankine. A high-quality combination multiplier-divider was used. The output signal from the multiplier-divider was then applied to an open operational amplifier, which incorporated an unsegmented nonlinear device in its feedback circuit for producing a square-root signal, as had been done for the liquid flow calculation. The resultant output was then

approximately proportional to the instantaneous vapor-flow rate and was sent to the strip chart recorder. The vapor-flow-rate signal together with its component parts were also displayed on panel meters at the test site for ready reference.

Pressure. - The pressure measurements, other than those connected with mercury-liquid- and vapor-flow measurement, are now described. Following the mercury flow through the system (fig. 5), the first pressure measurement was made in the relatively large-diameter outlet line leading from the large plenum at the boiler outlet. A 150-psia pressure pickup was connected to this static tap (P_5 station). Its output was processed for display at the test site with a panel meter so that the pressure level ahead of the condenser-inlet valve could be set for choked flow conditions.

The condenser-inlet static pressure was measured at the venturi outlet as shown in figures 5 and 7. The pressure transducer used was a high-temperature high-response flush diaphragm type, which was horizontally mounted and closely coupled (approximately $3\frac{1}{2}$ in.). The output signal was processed for recording on the strip chart recorder and for on site indication with a panel meter.

Another pressure measurement available in this experiment was that of the static-pressure drop across the outlet valve through which the condensate flowed. A differential pressure pickup was used which necessitated small lengths of connecting lines. The pickup and its lines were mounted at a slightly downward inclination from horizontal to avoid gas pockets in the chambered pickup once it and its lines were filled with liquid mercury. Hand valves and T's were incorporated in the lines for this purpose and for prerun calibration (detail, fig. 5). The processed signal was recorded with plus and minus capabilities on the strip chart recorder and indicated at the test site with a panel meter. Its measurement differential range was ±5 psi.

The monitoring of pressures throughout the mercury system was completed by incorporating a low-temperature absolute-pressure measuring pickup in the top of the receiver chamber to indicate the various pressure levels at which the condensate was exhausted. This variable was processed to a channel of the strip chart recorder and was indicated on site with a panel meter.

A differential pressure pickup was installed between the pipe supplying the coolant manifolds and the experimental chamber itself in order to repeat experimental runs at certain definite levels of nitrogen-coolant-flow rate. Its readings were calibrated originally against measurements made on a known orifice installed further upstream in the coolant supply line. Indication of the differential manifold pressure was on a panel meter available to the test-rig operator.

Interface position. - The high electric conductivity of liquid mercury was utilized in the following manner to ascertain the instantaneous interface position within small limits. Fusite pins, which are simply a metallic pin imbedded through a ceramic insulator around which is formed a metallic collar, were inserted through the top of the condenser

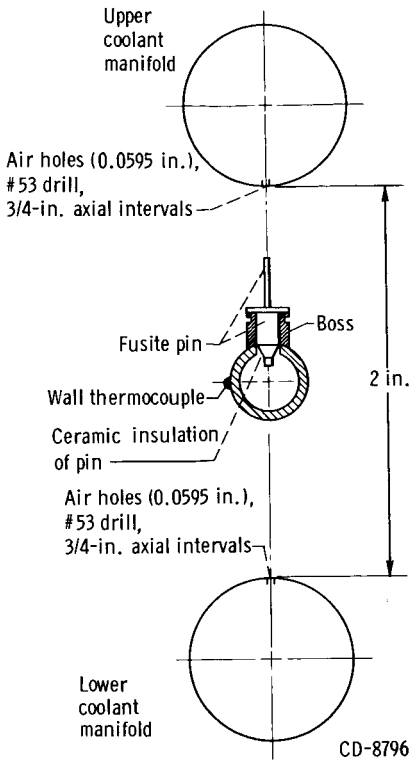

Figure 8. - Sectional view of condenser showing instrumentation details.

at 1-inch intervals along the downstream portion of the tube. The fusite collars were welded to bosses on the condenser in such a manner that the center pin extended inside the tube to approximately one-half the tube radius as shown in figure 8. When the liquid mercury in the tube reached the center pin, an electric conducting path was formed between it and the condenser wall. To indicate circuit closure, flashlight-type bulbs were inserted between each pin and a common voltage bus. This voltage bus was supplied from an electronically regulated low-voltage, high-current-capacity power supply with ground return connected to the condenser wall. The voltage level from this power supply was set at approximately 6 volts, which readily operated the lights yet was below the ionization potential of mercury vapor (about 15 V). The flashlight bulbs were mounted in an external rack to match the pin sequence, thus visual indication of interface position was provided.

The circuit shown in figure 9 was developed to provide capability for the instantaneous recording of interface position. The particular form that this circuit took is due to the following consideration. A small fluctuating resistance was observed between each pin and the condenser wall when the tube was filled with liquid mercury. This small resistance was attributed to the formation of a thin scale or oxide on the pin which occurred during use of the tube. This resistance is represented by the dotted resistance symbol in figure 9. Its effect was to make the voltage on the pin vary because of the potential divider action which occurred between the lamp bulb resistance and the small fluctuating resistance between pin and condenser wall. A differential, unstabilized, operational analog amplifier was employed with each pin to sense and to amplify the voltage drop occurring across each bulb as a result of current flow upon immersion of its corresponding pin in liquid mercury. When the liquid mercury in the tube did not immerse the tip of a pin, the resistance between pin and ground became extremely high, and, therefore, the potential at either end of the bulb was the same. For this condition, since the gain of each side of the differential amplifier was the same, the net amplifier output voltage was zero.

The output from each of the pin differential amplifiers was applied to a common summation point of another operational amplifier through individual summing resistance networks. These networks were included in the circuit design for the purpose of

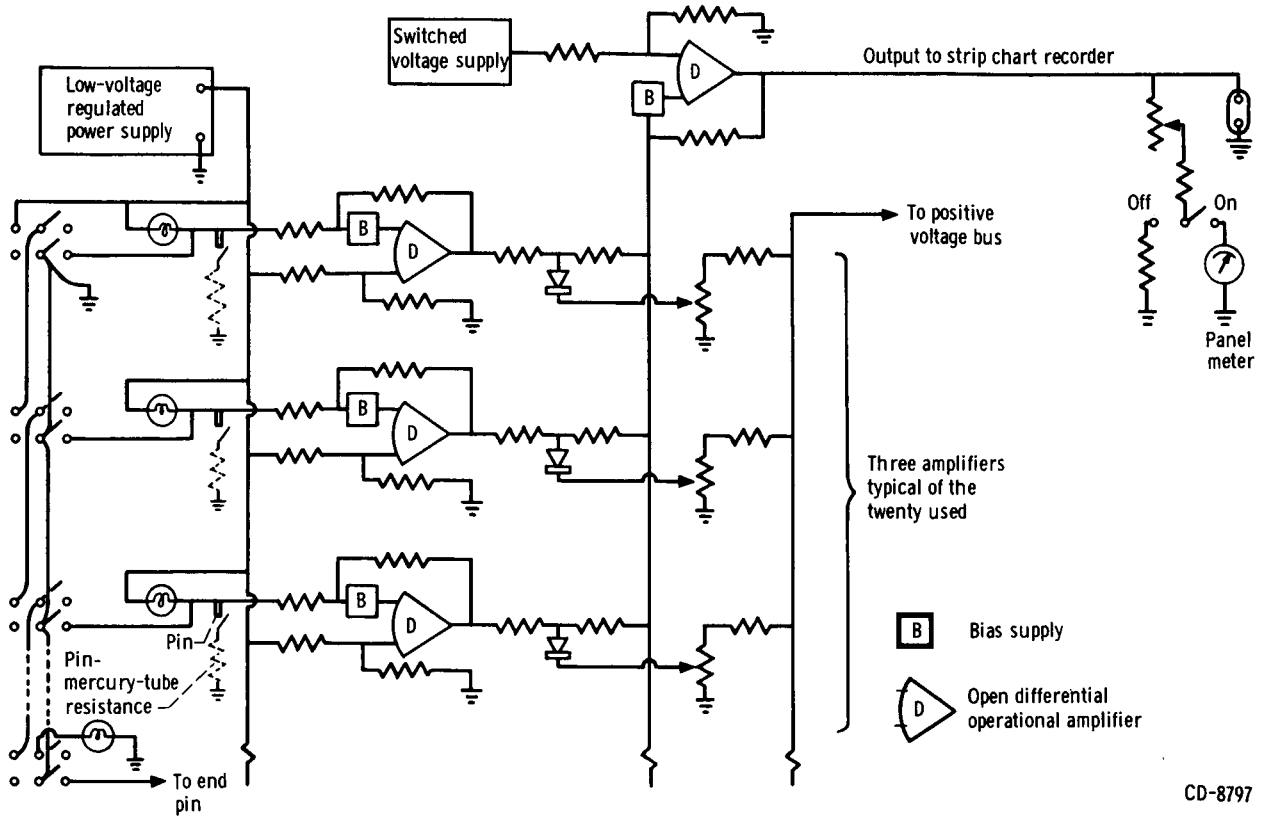

Figure 9. - Basic interface measuring circuit.

standardizing the magnitude of the output voltage from each pin operational amplifier before it was summed with other such voltages to produce an output voltage proportional to the number of closed-circuit pins. Each summation resistance network consisted of two resistors in series with a crystal diode connected between them and a potentiometer wiper. Each potentiometer was supplied from a common positive voltage bus with individual voltage dropping resistors connected in series. Leakage current resulting from the tapped-off potentiometer voltage was very small because of the high back resistance of the diode and could be compensated for by a slight adjustment of the bias supply incorporated with each operational amplifier. Therefore, the voltage applied to each resistor tied to the common summation junction of the output operational amplifier was zero, resulting in zero output to the strip chart recorder when no pins were immersed in liquid mercury.

Closure of a pin circuit by the liquid mercury in the tube allowed substantial current to flow through the light bulb thereby producing an appreciable voltage drop through it. This unbalance was applied to the pin operational amplifier through its summation resistors. The gain of each operational amplifier was set at a relatively high value so that closure of the pin circuit within wide limits resulted in a saturated output. This satu-

rated output voltage of positive polarity applied to the following summing resistance network allowed the crystal diode to conduct. The voltage appearing at the summation resistor attached to the common summation junction on the output operational amplifier, however, was held to that of the potentiometer wiper because of the relatively low resistance of the potentiometer. Thus, closure of a pin circuit over wide voltage limits resulted in the same definite adjustable voltage being applied to the output summation amplifier. As the liquid mercury interface swept up the tube, causing pin circuit closures, a staircase type of trace appeared on the strip chart recorder. Through adjustment of each potentiometer, every step was given an identical height. Switches were provided in parallel with the pins so that prerun calibrations of step height could be accomplished without any liquid mercury being in the tube. One side of each switch was tied through a series chain to an all-clear light bulb to insure that all switches were in the correct position before a data run.

A total of 20 pin amplifiers was used, resulting in a dynamic range of interface recording capability of 20 inches. Capability to record in regions other than the last 20 inches of the condenser was provided by a multigang switch, which selected what group of 20 pins would be sent to the pin operational amplifiers. Each switch position moved the measuring point another five pins upstream and simultaneously added in an appropriate voltage level from the switched voltage supply to the output operational amplifier to result in an equivalent shift of an additional five pins on the strip chart recorder. The voltage from the output operational amplifier was also monitored on site by a panel meter, which was a convenience during calibration.

Temperature. - Outside wall temperatures of the condenser were monitored with Chromel-Alumel thermocouples of fine wire spotwelded to the tube and covered with a very small amount of thermal insulation in the form of a cement to insure proper measurement in the presence of cooling gas flow. Spacing of the thermocouples varied but typically was at 3- or 6-inch intervals. The thermocouple reference lines terminated in a 150° F reference oven junction box from which copper lines carried the millivolt signals to a 28-point thermocouple selector switch as shown in figure 10. Position one of the switch was connected to read the T_{27} temperature, and the following switch positions followed the sequential arrangement of thermocouples down the condenser. The double wiper arm of the switch would feed any one of the signals to a high closed-loop gain differential amplifier, which amplified the millivolt signal to a usable level at low impedance.

As shown in figure 10, the output signal was routed to a meter circuit for on-site indication and to the strip chart recorder. The mechanical zero of the meter was set to match the 150° F position on a meter face plate modified to cover the range from 0° to 1000° F. This method obviated the incorporation of any biasing supply. A steady-state temperature profile could be obtained through scanning the thermocouples by manually

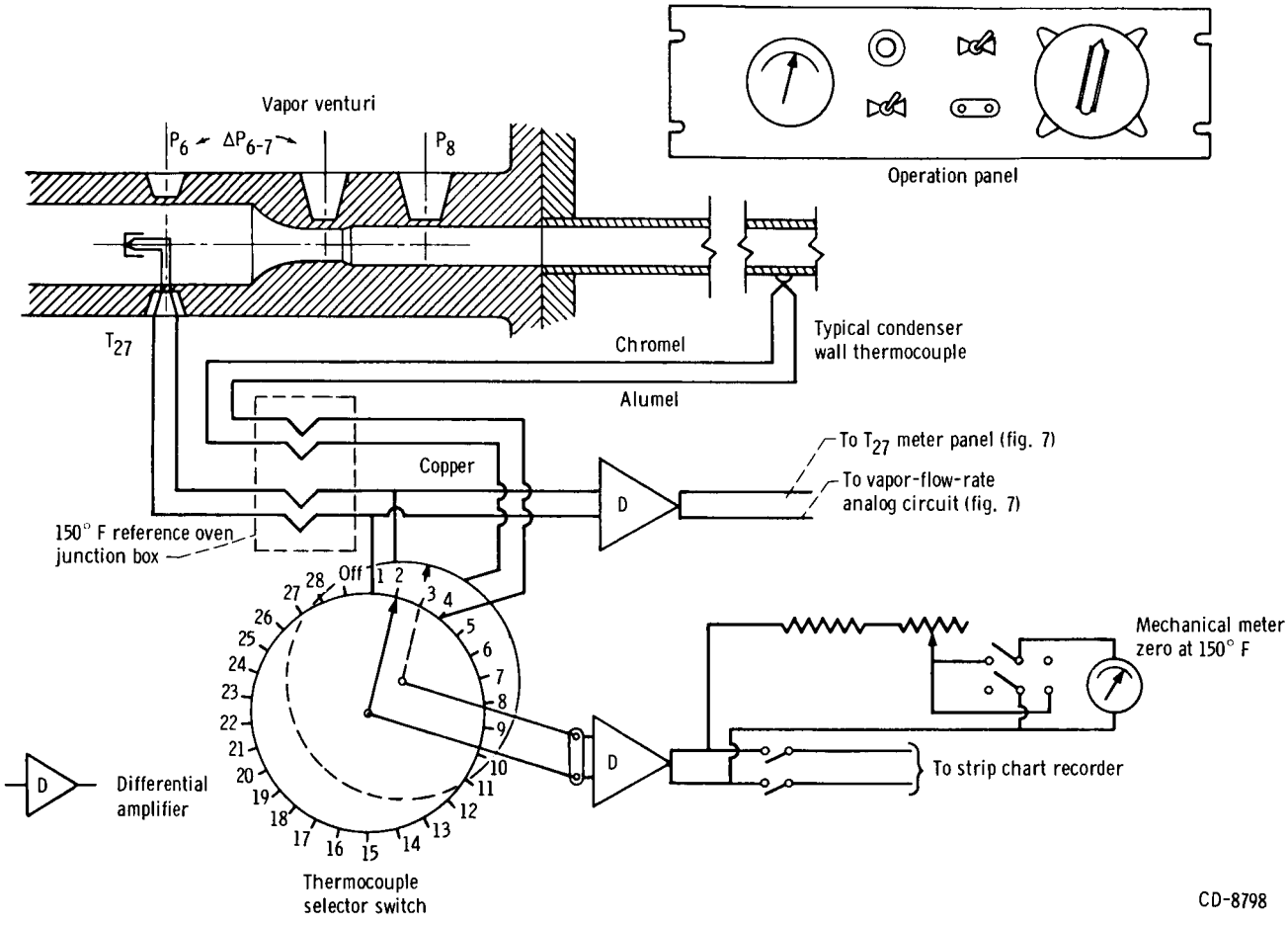

Figure 10. - Thermocouple scanning circuit for temperature profiles.

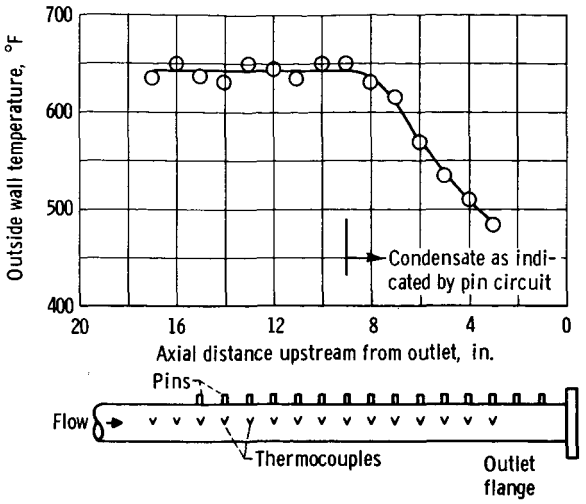

Figure 11. - Correlation of interface location between pin circuit and condenser-wall-temperature profile.

rotating the selector switch in sequence while the strip chart trace was moving at medium speed. A staircase type of trace of irregular height was obtained.

A typical wall-temperature profile obtained by this method is illustrated in figure 11. This figure also correlates the condensate interface located by the pin circuit and the interface location estimated by the sharp drop of condenser wall temperature which occurs in the region of condensate subcooling.

Valve position. - A battery-operated bridge type of circuit was devised for use in conjunction with the potentiometer mounted on either of the valve actuator shafts for position indication. The circuit is illustrated in figure 12. The resistance arms making up the bridge were of a significantly lower value than that in series with the meter, thereby producing a linear indication. This type of circuit allowed external calibration by making adjustments while observing movement of the meter pointer. Calibration was achieved when the meter movement would sweep between 0 and 100 percent travel as the valve was closed and opened. A signal proportional to the travel of the upstream valve was recorded on a channel of the strip chart recorder.

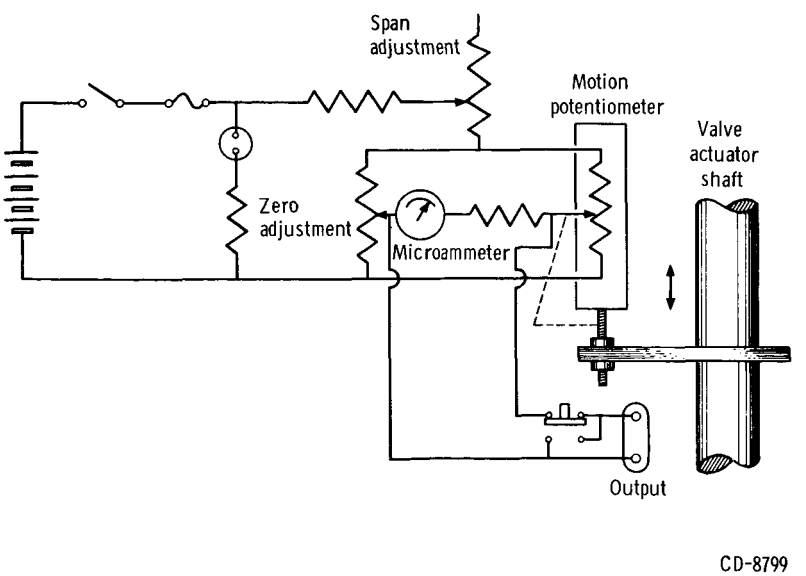

Figure 12. - Valve travel indicator circuit.

PROCEDURE

Calibration

Initially, the electric output from the absolute pressure pickups was zeroed by adjustment of the respective demodulators with the system under vacuum. Then a regulated adjustable supply of inert gas was used to pressurize the pressure pickups. The calibration pressure levels were monitored through use of accurate Bourdon gauges. With the appropriate pressures applied, the electric spans were set by adjustment of the respective attenuator following each demodulator. The output from each attenuator was amplified by means of a closed-loop differential amplifier having fixed gain settings. During attenuator adjustment, signals were monitored with an electronic digital voltmeter connected at the respective differential amplifier output. Outputs were standardized at a 10-volt level. This calibration procedure was followed to avoid the interaction which occurred between the zero and the span adjustments internal to the demodulator.

The differential pressure pickups and their lines were first filled with liquid mercury and then capped off from the system with handvalves. With both sides of each pickup open to atmosphere by way of the line T's, its electric output was zeroed. The appropriate gauge pressure was then established on the upstream tap of each pickup, and its span was set according to the procedure used for absolute pressure pickup calibration.

Following calibration of the ΔP_{1-2} pickup, the differential pressure corresponding to full system flow rate through the calibrated orifice was applied, and the spans were set on the W_L meter and on the recorder. The gauge pressure was then reduced and further cross checks were made.

In general, the output signal from each amplifier was displayed on a panel meter at the test site with the more pertinent ones being also recorded on the eight-channel strip chart recorder. The recorded pressure signals were P_8, ΔP_9, and P_R. Zero and span adjustments of meters and recorder followed or were simultaneous to electric calibration.

The display and recording of temperature signals necessitated a different procedure. As fixed gain operational amplifiers were used in connection with the thermocouples, only calibration of the readout equipment was necessary with the thermocouples terminated in a 150° F reference oven. If the measuring thermocouples were at the same 150° F temperature, there would be zero output. Accordingly, the meters used for temperature readout had the mechanical zeros set to the 150° F position with their electric circuits open, which is equivalent to having zero output from the junction. The recorder channel, set to read between 0° and 1000° F, also required that with zero input its pen should be set to the 150° F position. Recorder and meter spans were set after

disconnecting the electric lines to the respective differential amplifiers and in their place inserting a calibrated millivolt signal corresponding to a 1000° F thermocouple temperature. A commercial standard cell millivolt potentiometer was used as a signal source.

Calibration of the W_V analog calculation circuit involved substitution of a test patchboard from which were derived known voltages corresponding to various venturi pressures and temperatures. These same voltages were simultaneously sent to the on-site meters for further cross-checking. Monitoring of voltage levels at various points was by means of an electronic digital voltmeter. Following completion of any analog adjustments, the spans of the W_V readout meter and of the recorder channel were set.

The adjustments mentioned in the section Instrumentation were employed for calibration of the interface circuit. After each of the pin differential amplifiers was balanced by means of its bias supply, the offset resulting from the small diode reverse leakage currents could be nullified by adjustment of the increased biasing capability of the summation amplifier. Output nulling of the summation amplifier followed after the nulling of all 20 pin amplifier outputs. The electric switches were used to close each pin circuit proceeding upstream from the most downstream pin. Sequential adjustments of each step height were made. Following these adjustments, a check was made on the summation amplifier output as the selector switch was rotated, thereby supplying various bias levels from the switched voltage supply. These bias levels were then trimmed if necessary.

The procedure followed in calibrating each valve travel indicator was to fully close each valve by means of its valve drive circuit and then trim the zero adjustment potentiometer until the indicator would read zero. The valve was then opened, and the span was adjusted until the indicator read full scale. The upstream indicator circuit also supplied a signal for recording purposes.

The preceding calibration procedure was employed before each run.

Startup

Following calibration, the system was maintained under vacuum conditions as the mercury heaters were brought to operating temperature. Condenser inlet and outlet valves were both open during this period. The solenoid valve following the expulsion reservoir was opened, and a flow rate was initiated into the system by adjusting the inert gas pressure applied to the expulsion reservoir. After a period of time, the condenser-inlet valve was successively adjusted toward partial closure, which resulted in a slow buildup of plenum pressure. Simultaneously, the system-inlet flow rate was brought up to the desired level. Equilibrium conditions were sought at the desired flow level such that the plenum pressure would remain sufficiently high to maintain choked flow through the

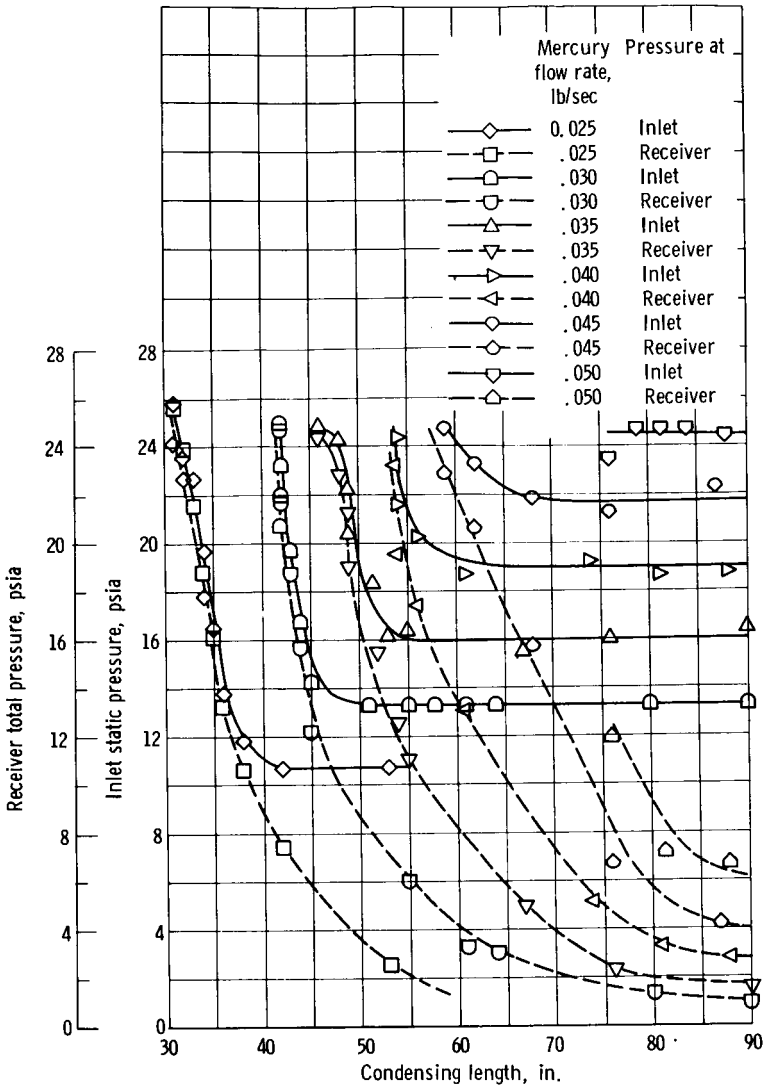

Figure 13. - Steady-state map at 0.089 pounds per second of coolant flow.

condenser-inlet valve over the expected test range. Allowance was made in available valve travel for manipulation of the valve about its set value.

The nitrogen cooling gas, which had been turned on during this period to ensure liquid at the condenser outlet, was adjusted to the desired flow rate for the particular run through manipulation of the nitrogen regulator while the ΔP_M meter was observed. Following this adjustment, the receiver pressure was gradually increased to give a desired interface position with consequent resultant condenser-inlet pressure level. Interface location was determined by the pin circuit lights when the interface was toward the rear of the condensing tube and by wall temperature scanning when the interface was further up the tube beyond the pin section. The presence of vapor pockets in the liquid

mercury in the tube was indicated by unlit pin lights. When this condition was observed, dynamic data, particularly that of interface movement, were not taken.

Steady-State and Dynamic Tests

Initial steady-state tests of the condenser disclosed two distinct regions of operation. That is, two distinct slopes were indicated for the curve of the inlet pressure against condensing length at given vapor- and coolant-flow values. Accordingly, experimental steady-state mapping of condenser performance was conducted by running at various vapor-flow and coolant-flow levels while the receiver back pressure was varied. Points were taken for various values of receiver pressure covering the range of 0 to 25 psia. A resultant map for a given coolant-flow rate is shown in figure 13. Selection of a distinct region of condenser operation wherein frequency response tests could be run was then made. Accordingly, tests could also be set up for the other distinct region.

For the dynamic tests, steady-state conditions were first set according to the known map. Then, nearly sinusoidal disturbances in inlet-vapor-flow rate about a given quiescent level were generated by supplying a sinusoidal voltage to the condenser-inlet valve drive amplifier from a low-frequency function generator. Use of the function generator allowed steps of the same amplitude as the sinusoid to easily be inserted as was necessary for gain normalization during data reduction. The lowest frequency available from the function generator was 0.01 cps. For some cases, a very low frequency generator was employed as an excitation source. However, at these very low frequencies, down to 0.001 cps, the varying outlet flow from the plenum and the accompanying pressure fluctuations began to be reflected through the entire boiling system even to the extent of causing a variation in system-inlet flow. A sample dynamic trace corresponding to 0.03 cps is presented in figure 14.

METHODS OF DATA REDUCTION

As a minimum, the dynamic recordings included the simultaneous variations of inlet valve travel, vapor-flow rate, and condenser-inlet pressure. In other cases, the dynamic recordings included the simultaneous variation in interface, and, in one case, the variation in static-pressure drop across the partially closed outlet valve through which the condensate flowed was also obtained. The typical low-frequency recording (0.03 cps), presented in figure 14, illustrates the general waveform shapes obtained for the dynamically varying quantities. This figure shows the sinusoidal inlet valve travel movement and resultant inlet vapor flow to the condenser. The amplitude of valve travel movement

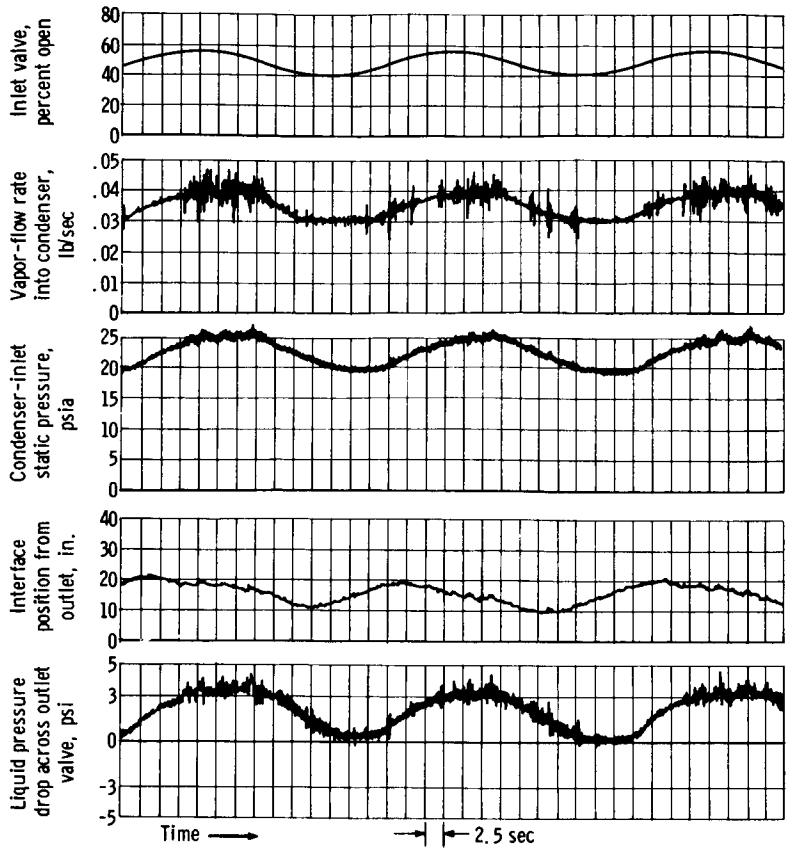

Figure 14. - Low-frequency recording illustrating various waveforms encountered.

was set to produce about ±10-percent variation in inlet-vapor-flow rate. This variation resulted in an appreciable swing in condenser-inlet pressure and interface movement at the low frequencies. The very high-frequency fluctuations observable in the vapor-flow rate waveform are attenuated by the system and do not reflect into the other traces. This figure indicates a reasonable sine wave in pressure but distortion in the interface waveform. Note the individual stepped nature of the interface waveform as given by the pin circuit yet its overall continuous analog appearance. The overall interface waveform is observed to have a steep rise when moving up the tube and to have a gradual slope when retreating toward the outlet. This characteristic is attributed to a secondary build-up of the amount of condensate due to the fact that the interface absorbs all drops and runoff inside the tube as the interface moves forward. When the interface retreats down the tube, it tends to become ragged and leave drops and runoff behind.

The condenser-inlet pressure trace, relative to that of the disturbance vapor-flow rate, exhibited only a small phase shift over the frequency range covered and would, therefore, require accurate phase determination to avoid data scatter. The existence of significant interface waveform distortion suggested that direct reading of the traces

would not be accurate. Accordingly, two other methods were generally employed. These methods were a reference trace overlay method and a Fourier analysis method. Selection of a method depended on the waveforms to be processed. For the case where only the dynamics of condenser-inlet pressure relative to vapor-flow rate were concerned, the reference overlay method was used. This choice was based on the fact that the waveform of condenser-inlet pressure and vapor flow exhibited relatively low distortion, and the reference overlay method would be adequate under these conditions. The reference overlay method was also less time consuming.

When the interface was also available, the traces were generally processed by employing the Fourier analysis method. Either method required use of recorded valve travel position as a reference for determining the exact length of a cycle since the waveform of valve position was reproduced exactly from cycle to cycle whereas that of the vapor-flow rate was distorted a varying amount from cycle to cycle. The methods of waveform processing are discussed in detail in the appendix.

The typical data processing procedure was as follows: An average W_L value was read from the chart recording together with the high and low reading of the W_V sinusoid, which had been drawn in by the trace overlay method. An average vapor-flow rate $\overline{W}_V$ and differential ΔW_V were calculated from these high and low readings. Sometimes the $\overline{W}_V$ reading was observed to be slightly greater than that of the W_L reading. As the W_L reading was believed more accurate, the ΔW_V value was divided by the ratio $\overline{W}_V/W_L$ to arrive at a corrected quantity ΔW_{VC}. Similarly, the high and low readings of the P_8 sinusoid, which had also been drawn in by the trace overlay method, were read. The average pressure level $\overline{P}_8$ and differential ΔP_8 were calculated. The ratio of pressure change to flow change $\Delta P_8/\Delta W_{VC}$ was then calculated. This ratio was normalized to the corresponding steady-state ratio by dividing by the appropriate normalization.

A normalization value of 545 was obtained, for example, from the experimental step responses of figure 15. The asymptotic tailoff of each step response supplies data above and below the operating level at which the frequency response tests were run. Accordingly, values of pressure and flow were read on the tailoff just preceding the next step input. The points read are as follows:

First step

$$\frac{\Delta P_8}{\Delta W_V} = \frac{22.8 - 14.8}{0.0495 - 0.0348} = 544$$

Second step

$$\frac{\Delta P_8}{\Delta W_V} = \frac{19.0 - 14.8}{0.0425 - 0.0348} = 546$$

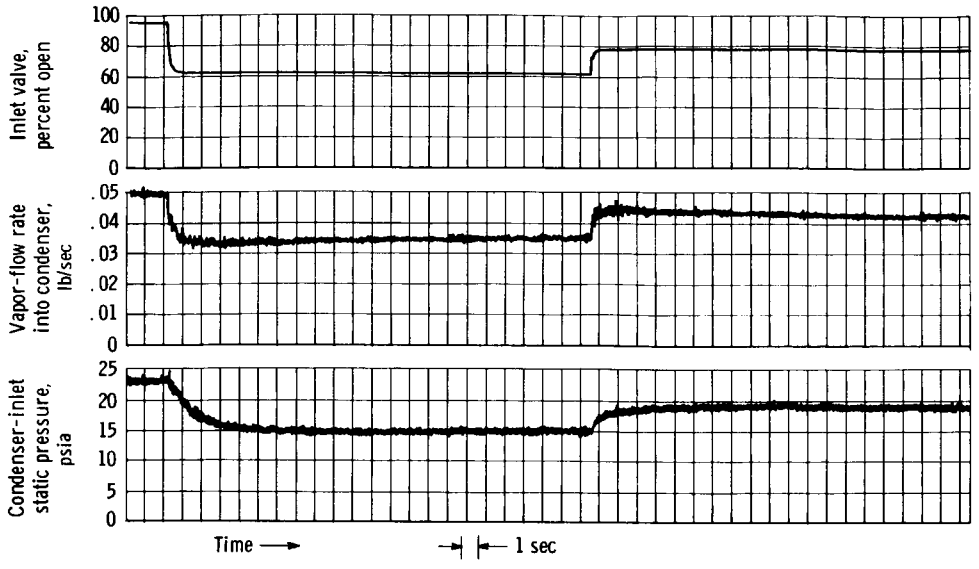

Figure 15. - Step response of pressure to flow used in normalizing frequency response data of figure 17.

The normalization number of 545 compares very closely to the value of $\Delta P_8/\Delta W_V = 565$ as obtained by cross-plotting corresponding steady-state data from the condenser map of figure 13 (p. 18). The cross plot is shown in figure 16.

The previous procedure was adequate to a frequency of 1 cps. Actuation of the upstream valve at higher frequencies resulted in an erroneous rise in the vapor-flow-rate indication. That is, as the driving frequency was increased, the differential of valve travel began to decrease, whereas the differential of the measured vapor flow began to increase even though the flow was supplied from a constant-pressure plenum under choked conditions. This effect was observed to occur with the system cold (and consequently without flowing any mercury vapor) and was traced to the ΔP_{6-7} measurement. This pickup, as had previously been mentioned, required liquid mercury in the lines leading to its diaphragm chamber. The rig, which was suspended by wires to allow for thermal expansion, shook sufficiently with actuation of the upstream valve to produce a sinusoidal variation in the output from the ΔP_{6-7} pickup. Although a resonance occurred at 6 cps, there was no appreciable effect at 2 cps and, therefore, negligible effect at lower frequencies. Accordingly, as the pressure level ahead of the cycling valve was constant, the ratio $\Delta W_{VC}/\Delta VT$ was determined at each test frequency over the range 0.01 to 1 cps. An average ratio for this interval was determined. Then starting at 1 cps and going to higher frequencies the differential of

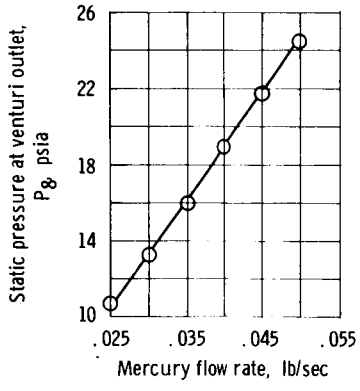

Figure 16. - Cross plot of steady-state map at 0.089 pound per second coolant flow (fig. 13) for alternate gain determination of 565 seconds per square inch.

valve travel ΔVT was multiplied by this averaged ratio to get an equivalent differential flow change $\Delta W'_{VC}$. The ratio of $\Delta P_8/\Delta W'_{VC}$ was calculated next. This ratio was in turn normalized as had been done in the low-frequency region. For all frequencies, the phase determination was done at the time of application of the trace overlay method to the various waveforms. Phase indication above 5 cps was uncertain because of the large overriding phase shift of the resonance occurring at 6 cps.

RESULTS AND DISCUSSION

The form of the response of condenser-inlet pressure to vapor-flow rate was observed to be different in the different regions of the steady-state map that relates the inlet static pressure and receiver pressure to condensing length at various constant flow rates. The significant difference between the two regions of a map is that of the sensitivity of inlet pressure to interface position. This sensitivity may be seen by examining the steady-state map presented in figure 13 (p. 18). Each curve of inlet static pressure and condensing length is characterized by a region of high slope (negative) at the short lengths and a region of practically zero slope at the long lengths. The transition between these regions, or knee of the curve, is rather sharp. Condensing length, of course, is the difference between tube length and interface position. The region of high slope, or high sensitivity, is also a region of small overall two-phase pressure drop, while the region of low slope, or low sensitivity, is a region of large two-phase pressure drop. This fact was ascertained from the maps as follows: Tests showed the liquid pressure drop (from the interface to the receiver) to be approximately 0.2 psi, which was below the accuracy range of the transducers and was measured with inclined manometers. The pressure at the interface was, therefore, just slightly above that of the receiver. In the short condensing length region, the inlet static pressure was nearly the same as that of the receiver; therefore, the two-phase pressure drop was small. As the condensing length was increased by lowering the receiver pressure, a lower limit was eventually reached for the condenser-inlet pressure, and the two-phase pressure drop thereafter became appreciable.

Pressure Response in Region of Low Sensitivity to Interface Position

Dynamic tests were run at different levels of heat flux for approximately the same condensing length. The operating conditions for the high heat-flux rate were a vapor-flow rate of 0.040 pound per second and a 13-inch approximate interface position as a result of the 0.089-pound-per-second coolant flow. The corresponding steady-state map

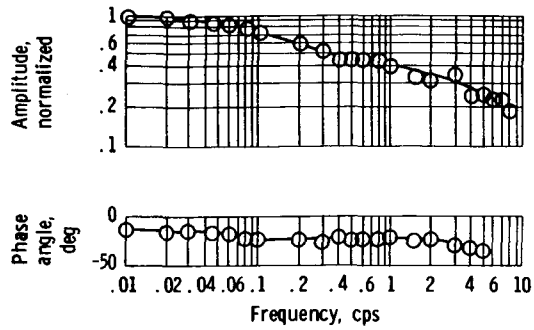

Figure 17. - Response of inlet static pressure to vapor-flow cycling. Vapor-flow rate into condenser, 0.040 pounds per second; average condenser-inlet pressure, 19.1 psia; total pressure in receiver, 4.6 psia; interface position, 13 inches; differential pressure of coolant, 5.0 psi; flow rate into manifold, 0.089 pound per second.

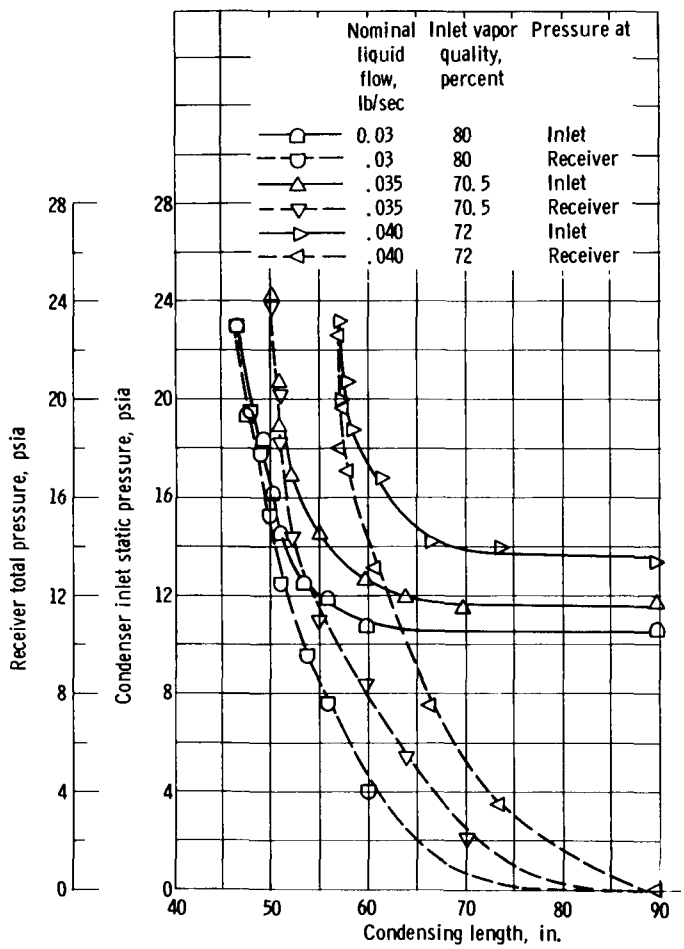

Figure 18. - Steady-state map at coolant flow of 0.033 pound per second.

is presented in figure 13 (p. 18). The operating region is observed to be well inside the region of low sensitivity. The resultant frequency response data is presented in figure 17. The form of the response given in figure 17 is that of an overdamped system since the amplitude ratio does not rise above 1 and the phase shift is always lagging. This response form is also observable in the step response of figure 15. The response to a step change in flow is of a lagging nature and is completely without overshoot.

Since normalized amplitude ratio and relative phase shift are presented as a function of frequency in figure 17, it is in reality a Bode plot. Comparison may be made to a variety of accumulated Bode plots for known transfer functions available in controls literature. The data in figure 17 approximate the Bode plot of a lag-lead-lag transfer function (ref. 3).

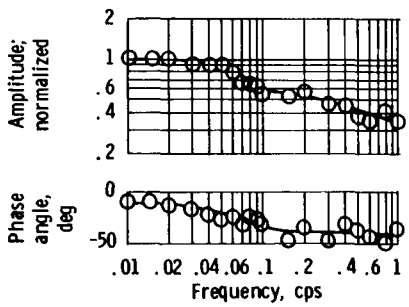

Figure 19. - Response of inlet static pressure to vapor-flow cycling. Averaged vapor-flow rate into condenser, 0.03 pound per second; average condenser-inlet pressure, ≈ 15 psia; total pressure in receiver, 8.8 psia; average interface position, 15 inches; differential pressure of coolant, 1.0 psi; flow rate into manifold, 0.033 pound per second.

The theoretical basis for the form of condenser response and the variation of form with operating point is given in reference 2.

Similar dynamic tests were also run at a low heat-flux rate. The operating conditions for these tests were a vapor-flow rate of 0.030 pound per second and a nominal condensing length of 75 inches. This required reduction of the coolant flow rate to 0.033 pound per second. This steady-state map is presented in figure 18. The map data was not available at 100-percent quality because of a shift in boiler performance. Nevertheless, the region of operation regarding the inlet-pressure - interface sensitivity may be identified from the values of condenser-inlet pressure and receiver pressure recorded at the inception of the frequency response tests. These pressures are 15 and 8.8 psia, respectively, indicating a large two-phase pressure drop and, hence, operation in the low-sensitivity region. The resulting pressure frequency response plot is presented in figure 19. Although the two-phase pressure drop is less than half of that of the previous condition (cf. operating condition in fig. 17, p. 24) and the heat flux was reduced about 25 percent, the pressure response of figure 19 has the same characteristic shape as that of figure 17. Within this region, therefore, variations of the heat flux and the two-phase pressure drop did not materially affect the form of the condensing pressure frequency response.

Effect of Pressure Sensitivity to Interface Position

The effect of increased pressure sensitivity to interface position was next investigated. The steady-state conditions of 0.035-pound-per-second vapor flow, 50-inch condensing length, and 0.089-pound-per-second coolant flow put the operating point in the region of high sensitivity (cf. previous map, fig. 13, p. 18). Under these conditions, the two-phase pressure drop is small. The normalized frequency response plot of pressure to vapor flow is presented in figure 20. A normalization value of 150 was obtained from the experimental step response of figure 21. As was done previously, values of pressure and flow were read on the asymptotic tailoff just preceding the next step input. The points read are as follows:

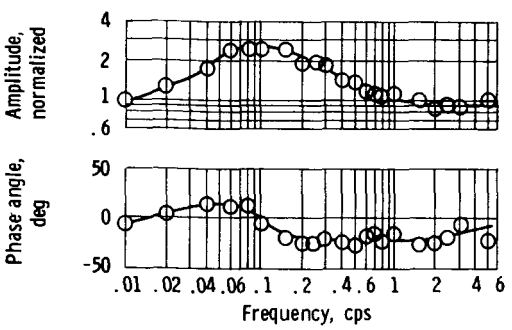

Figure 20. - Response of inlet static pressure to vapor-flow cycling. Averaged vapor-flow rate into condenser, 0.035 pound per second; average condenser-inlet pressure, 20.3 psia; total pressure in receiver, 18.7 psia; average interface position, 40 inches; differential pressure of coolant, 5.0 psi; flow rate into manifold, 0.089 pound per second.

$$\frac{\Delta P_8}{\Delta W_V} = \frac{20.4 - 19.5}{0.0395 - 0.0335} = \frac{0.9}{0.006} = 150$$

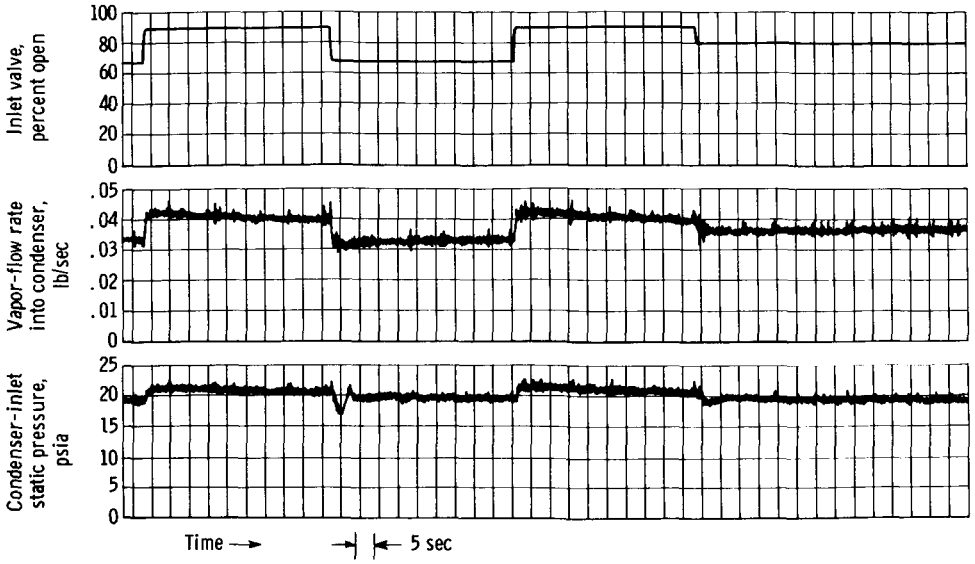

Figure 21. - Step response of pressure to flow used in normalizing frequency response of figure 20.

The transient response to a step input varied with step size and direction and, thus, indicated nonlinearities.

The response form of figure 20 is considerably different from the forms in figures 17 and 19. Whereas, the previous normalized amplitudes were of an attenuating nature (i.e., less than or equal to 1), the normalized amplitude response for this condition rises above 1 to a peak of 2.6 at approximately 0.1 cps. The phase shift characteristic is also significantly different from the responses obtained in the low-sensitivity region. Whereas the other responses had been of a lagging nature only, the phase characteristic in the high-sensitivity region was of a leading nature over the frequency range 0.01 to 0.1 cps. At frequencies greater than 0.1 cps, the phase reverts to a continuously lagging nature. These amplitude and phase characteristics approximate those of a lead-lag-lag transfer function. The Bode plot of a lead-lag transfer function is demonstrated in reference 4. A lead-lag-lag transfer function would have a similar Bode plot at the low frequencies but with additional attenuation and more phase lag at the high frequencies.

It can be concluded, therefore, that the two distinct regions of condenser operation, identifiable by high or low sensitivity of inlet pressure to interface position, have markedly different response forms of inlet pressure to vapor flow.

Effect of Liquid Resistance

The effect of increasing the liquid pressure drop by partially closing the condenser-outlet valve was also investigated. In figure 22, the condenser-inlet pressure response

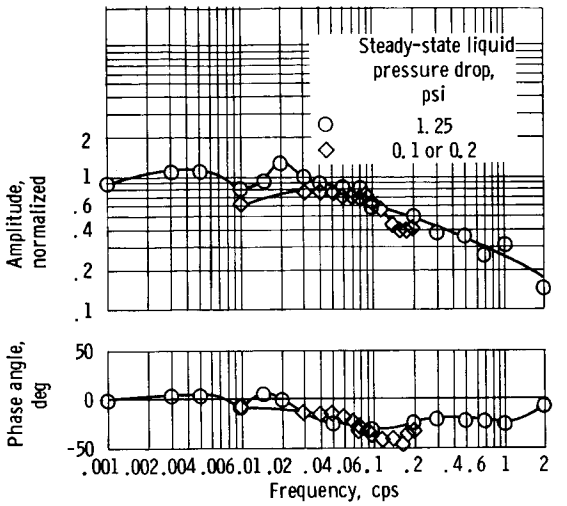

Figure 22. - Response of condenser-inlet pressure to inlet vapor flow for two different outlet valve settings. Averaged vapor-flow rate into condenser, ≈0.035 pound per second; average condenser-inlet pressure, ≈22.2 psia; total pressure in receiver, ≈18.4 psia; average interface position, ≈15 inches; differential pressure of coolant, 1.0 psi; flow rate into manifold, 0.033 pound per second.

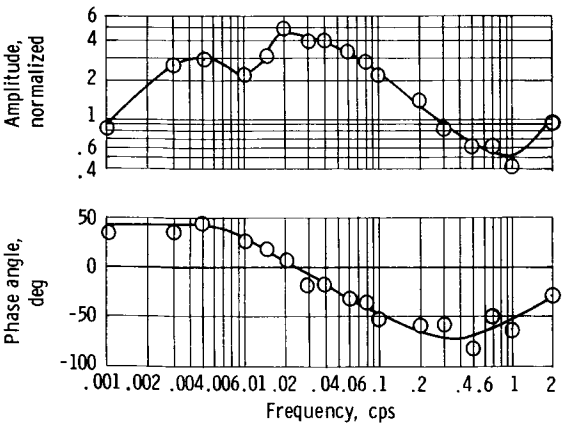

Figure 23. - Response of static-pressure differential across the condenser-outlet valve when set for a quiescent level of 1.25 psi. Liquid-mercury flow rate, ≈0.035 pound per second; differential pressure of coolant, 1.0 psi; average condenser-inlet pressure, ≈22.2 psia; total pressure in receiver, ≈18.4; average interface position, ≈15 inches; flow rate into manifold, 0.033 pound per second.

at 0.033-pound-per-second coolant flow is presented. Two sets of data are superimposed. The one set is for the outlet valve wide open, which produces a liquid pressure drop of 0.1 or 0.2 psi. The other set is for a steady-state liquid pressure drop of 1.25 psi across the partially closed outlet valve. The mean operating conditions for these tests were a flow rate of 0.035 pound per second at about 100-percent quality with an approximate 75-inch condensing length. The inlet and receiver pressures were 22.2 and 18.4 psia, respectively. The closeness of these pressures results in operation at the inlet pressure knee of the steady-state map. The increase in liquid resistance is observed to have a small effect on the inlet pressure response. An increase in the liquid resistance tends to produce a peaking in the pressure response. This effect may be explained by noting that increasing the liquid pressure drop moves the operating point further up the knee on a steady-state map and, thus, to higher sensitivity of inlet pressure to interface position. As in figure 20, therefore, a peaking in response is to be expected, but the peaking is relatively small in the present case because operation is in the transition region.

For the operating condition wherein the outlet valve was partially closed, an appreciable variation in differential pressure occurred across the outlet valve. The normalized response of this differential pressure is given in figure 23. As there is a constant receiver pressure and only a small liquid pressure drop other than through the valve, this plot can be taken as an approximate pressure response at the interface.

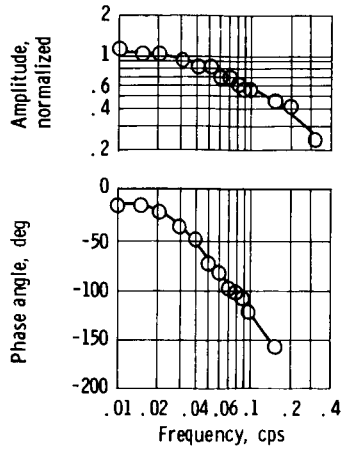

Figure 24. - Response of condensing length to vapor-flow cycling based on available half-wave waveform. Averaged vapor-flow rate into condenser, 0.03 pound per second; average condenser-inlet pressure, ≈15 psia; total pressure in receiver, 8.8 psia; average interface position, 15 inches; differential pressure of coolant, 1.0 psi; flow rate into manifold, 0.033 pound per second.

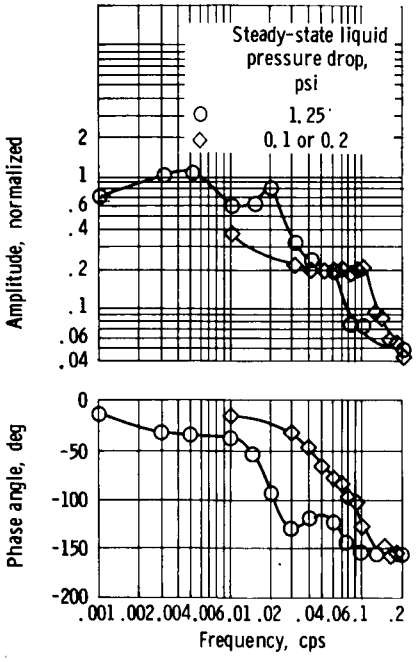

Figure 25. - Response of condensing length to inlet vapor flow for two different outlet valve settings. Average vapor-flow rate into condenser, 0.035 pound per second; average condenser-inlet pressure, ≈ 22.2 psia; total pressure in receiver, 18.4 psia; average interface position, ≈15 inches; differential pressure of coolant, 1.0 psi; flow rate into manifold, 0.033 pound per second.

The general shape of the amplitude characterisitic is seen to be similar to that of the inlet pressure.

Interface Response

For some cases, it was possible to monitor the variation in interface position concurrent with the variation in condenser-inlet pressure which resulted from vapor-flow cycling. Presented in figure 24 is the interface response, which occurs concurrently with the response in condenser-inlet pressure as given in figure 19 (p. 24). A value of 2100 inches per pound per second was employed in normalizing this response. Because of instrumentation limitations for this run, the wave form obtained was only half-wave thereby voiding application of Fourier analysis. The data, however, indicate interface response under conditions which correspond to the region of low sensitivity of inlet pressure to interface position. The response is seen to be of a continually attenuating nature with simultaneously a large increase in lagging phase shift. This characteristic is similar to an overdamped second-order system (ref. 3, pp. 311 and 313).

The interface response, under the conditions which correspond to being on the knee of the steady-state map wherein there is an increased sensitivity of inlet pressure to interface position, is shown in figure 25. These data were obtained simultaneously with those shown in figures 22 and 23. Here the amplitude response for the case where the outlet valve was open (0.1- to 0.2-psi differential liquid pressure drop) levels off between 0.04 and 0.1 cps; thus, less of an overdamped response was indicated than was the case for the low sensitivity region (fig. 24). Included in figure 25 is the effect on interface response of artificially increasing the liquid pressure drop. A rise in response is indicated at 0.02 cps, which matches that of the condensing pressure response (fig. 22) and

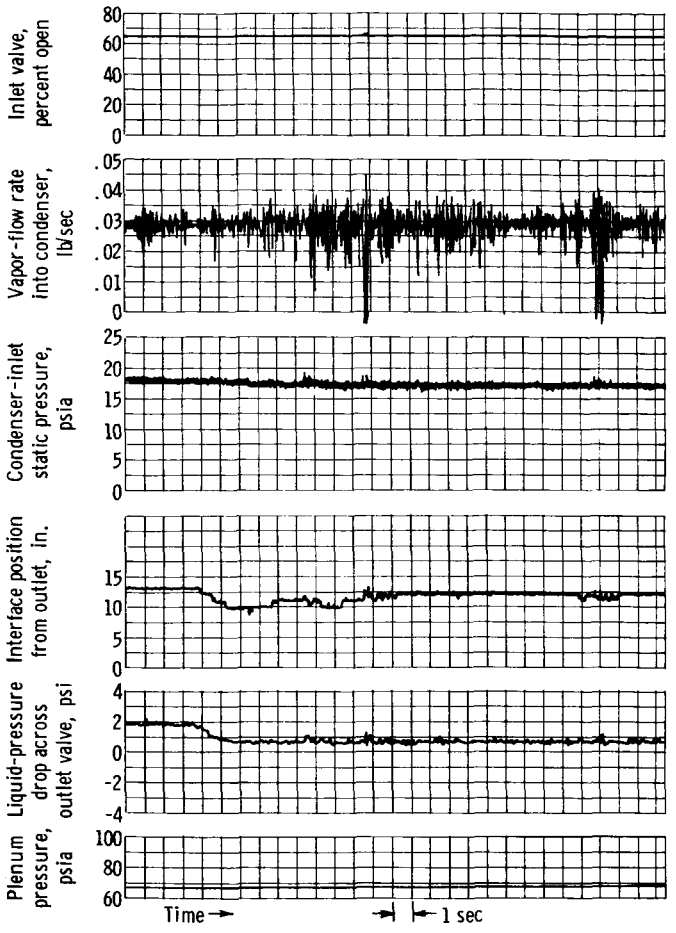

Figure 26. - Effect of rapid reduction in outlet liquid pressure drop.

liquid pressure drop across the outlet valve (fig. 23). The overall response of amplitude and phase were shifted to lower frequencies.

Under all conditions tested, the interface response attenuated rapidly at a relatively low frequency so that above this range the interface could be considered as being fixed during high-frequency flow cycling with resultant inlet pressure changes.

Instabilities

Several additional aspects of condenser operation were also noted. The effect of rapidly reducing the liquid pressure drop by opening the outlet valve is shown in figure 26. The interface and the condenser-inlet pressure readjust without any instability.

The effect of rapidly ramping the receiver pressure is displayed in figure 27. In an upward ramp as the receiver pressure exceeds the condenser-inlet pressure, the condenser-inlet pressure and the interface position break into oscillation. The frequency of this oscillation, 0.45 cps, is about double the observed self-oscillation frequency of 0.25 cps that occurs during condenser operation in which there is no outlet restriction. The effect of a ramp downward in receiver pressure produced no instability.

The effect of an abrupt change in flow when operating at an off-design condition is shown in figure 28. A small amount of pressure drop was supplied by the outlet valve even though open. Temporary instability in condenser-inlet pressure with attendant oscillation in interface position occured at 0.25 cps, correlating with the self-oscillation frequency.

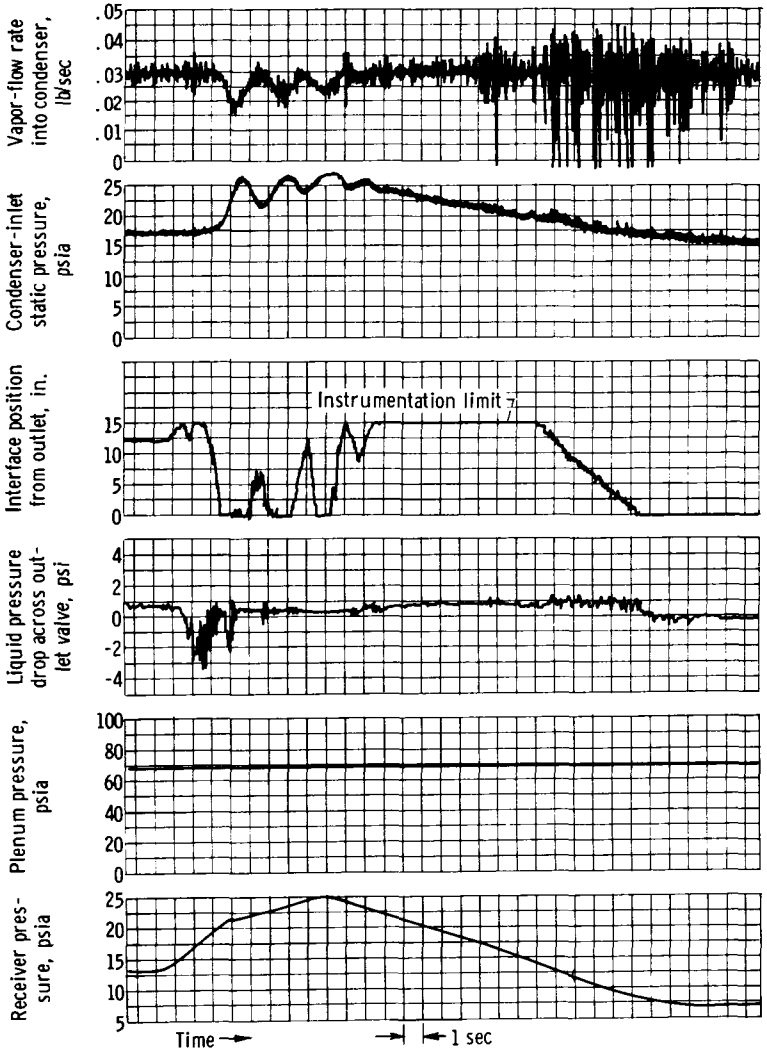

Figure 27. - Effect of ramping receiver pressure.

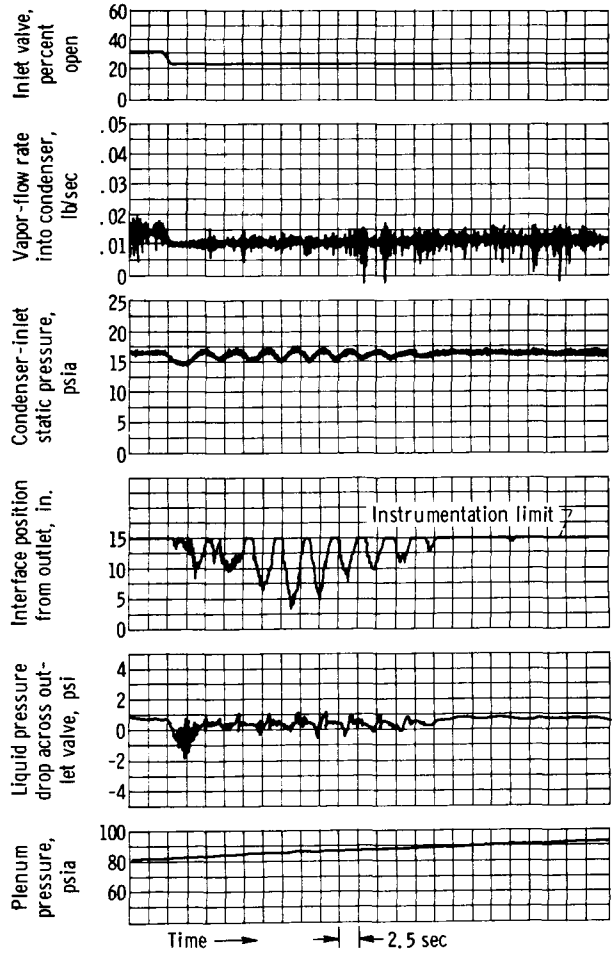

Figure 28. - Effect of abrupt change in flow at off-design condition.

SUMMARY OF RESULTS

This experiment obtained condenser dynamic information relative to a disturbance in inlet-vapor-flow rate. Through use of a constant-pressure receiver, the interface location was allowed to vary simultaneously in response to changes in condensing pressure. Under these conditions, the following results were obtained.

1. The condenser was observed to have two distinct regions of operation, identifiable by high or low sensitivity of inlet pressure to interface position. The response of condenser-inlet pressure to vapor-flow rate was observed to be different in each of the regions.

2. In the region of low sensitivity, the frequency response data of condenser-inlet pressure to vapor-flow rate indicated an approximate lag-lead-lag characteristic. Within this region, variations of the heat flux and two-phase pressure drop did not materially affect the form of the condenser pressure frequency response.

3. In the region of high sensitivity, the frequency response of condenser-inlet pressure to vapor-flow rate indicated an approximate lead-lag-lag characteristic.

4. The frequency response of interface position to vapor-flow rate indicated an approximate overdamped second-order system in the region of low sensitivity of inlet pressure to interface position and in the transition region between low and high sensitivity.

5. The effect of increasing the liquid pressure drop resulted in the interface response shifting to lower frequencies.

Lewis Research Center,
National Aeronautics and Space Administration,
Cleveland, Ohio, January 10, 1967,
701-04-00-02-0P0216.

APPENDIX - METHODS OF WAVEFORM PROCESSING

A description of the two methods employed for the processing of recorded waveforms is now given. Either method required use of recorded valve travel position as reference for determining the exact length of a cycle since the waveform of valve position was reproduced exactly from cycle to cycle, whereas that of the vapor-flow rate was distorted a varying amount from cycle to cycle.

The trace overlay method was used to process traces where only the response of condenser-inlet pressure relative to vapor-flow rate was available. Use of this method was possible because the waveform of condenser-inlet pressure had a low amount of distortion. The waveform of valve position, however, was a good representation of a sinusoid except at very high driving frequencies and had about the same amplitude as that of the vapor-flow rate and the inlet pressure. In the reference trace overlay method, a sheet of tracing paper was placed over the valve position recording, and the waveform was traced together with the cycle limits. The tracing was then overlaid on the vapor-flow-rate waveform and adjusted to balance out the distorted area above and below this waveform. The tracing was then taped and a carbon paper inserted underneath. A hard pencil was used on the tracing to transfer the valve travel reference waveform. The cycle limits were also transferred. The phase shift between the flow and the valve travel was determined by measuring the full cycle length and the length between cycle limit marks of the waveform relative to that of the valve travel waveform. The ratio of lengths multiplied by 360° was then the phase shift in degrees. The superimposed waveform was used as a pattern, and a new slightly larger or smaller sinusoid was sketched in to match the amplitude of the vapor-flow-rate waveform. The high and the low values of this sinusoid were read, and the net amplitude difference was obtained. This same procedure was then applied to the condenser-inlet-pressure waveform. The ratio of the amplitude of the pressure to the flow was then taken. The net phase shift was obtained by subtracting that of the pressure relative to the valve travel from that of the vapor-flow rate relative to the valve travel.

The Fourier analysis method was graphical and similar to that given in reference 5. The valve travel was used to obtain the exact length of one cycle, and the two lines corresponding to the start and the finish of the reference waveform were drawn perpendicular across the chart through the various distorted waveforms to be analyzed. The waveforms were then traced to eliminate the very high-frequency noise. The cycle limit lines of the reference waveform were also traced. Then each waveform was divided into a number of equal intervals between these cycle limit lines, either 72 (every 5° for long waveforms) or 36 (every 10° for short waveforms). Only the procedure for 5° intervals will now be described.

The height of each interval line from the zero reference base was measured and was

recorded sequentially under a column marked ORD (ordinate) on prepared work sheets. These work sheets also had columns marked SIN, SINORD, COS, COSORD. The sin and cos values corresponding to each 5^{o} interval were preprinted on each sheet under the appropriate SIN and COS columns. The direct component and fundamental sinusoid values were generally determined. The direct component value was obtained by taking one-half of the value of the ordinate at 0^{o} and at 360^{o} and summing with all the rest of the remaining ordinate values. The summation was divided by 72 to give the direct component value of the waveform.

The fundamental sinusoid was first determined by multiplying the numbers in the ORD column by the numbers given in the SIN column and recording them in the SINORD column. Likewise, the numbers in the ORD column were multiplied by the numbers in the COS column and were recorded in the COSORD column. Then all SINORD and COSORD terms were summed, and a quantity R was then calculated according to the relation

$$R = \sqrt{\left(\frac{\text{SINORD}}{36}\right)^2 + \left(\frac{\text{COSORD}}{36}\right)^2}$$

The quantity R was then one-half the peak-to-peak value of the sinusoid. The scale factor was then applied to this value to shift back in terms of the process variable. The phase θ is given by

$$\theta = \tan^{-1} \frac{\sum \text{COSORD}}{\sum \text{SINORD}}$$

The resulting phase shift was relative to the reference waveform as were the rest of the analyzed waveforms. The relative phase between any two channels was then simply the difference between the phase of each channel relative to that of the reference waveform.

A sample recording is shown in figure 29 together with its tracings and the resultant plots of each waveform direct component and fundamental sinusoid component as determined by the Fourier analysis method.

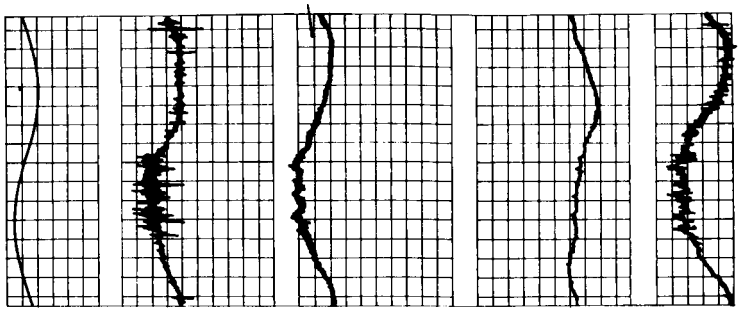

(a) Recorded waveforms.

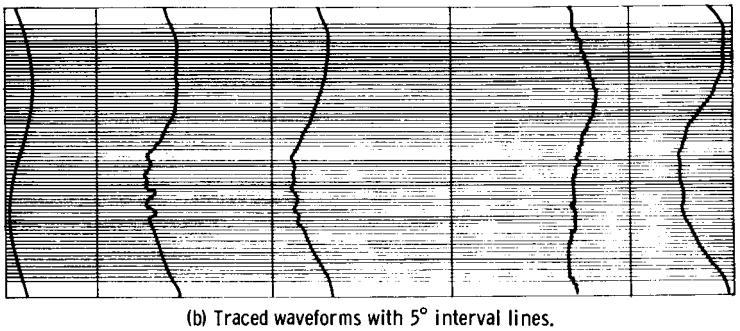

(b) Traced waveforms with 5° interval lines.

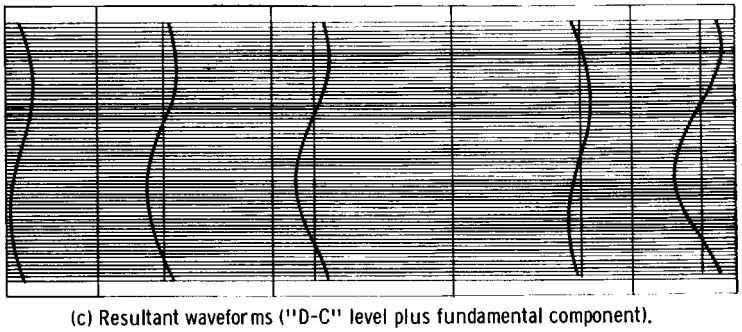

(c) Resultant waveforms ("D-C" level plus fundamental component).

Figure 29. - Illustration of the application of Fourier analysis to waveforms encountered.

REFERENCES

1. Packe, Donald R.; Schoenberg, Andrew A.; Jefferies, Kent S.; and Tew, Roy C.: Analysis of Condensing Pressure Control for SNAP-8 System. NASA TM X-1192, 1966.

2. Schoenberg, Andrew A.: Mathematical Model with Experimental Verification for the Dynamic Behavior of a Single-Tube Condenser. NASA TN D-3453, 1966.

3. Chestnut, Harold; and Mayer, Robert W.: Servomechanisms and Regulating System Design. Vol. 1. John Wiley and Sons Book Co., Inc., 1951, pp. 308, 311, and 313.

4. Brown, Gordon S.; and Campbell, Donald P.: Principles of Servomechanisms; Dynamics and Synthesis of Closed-Loop Control Systems. John Wiley and Sons Book Co., Inc., 1948, p. 268.

5. Kerchner, Russell M.; and Corcoran, George F.: Alternating-Current Circuits. Third ed., John Wiley and Sons Book Co., Inc., 1951, pp. 171-180.